Journal of Fundamental and Applied Sciences

Research Article

ISSN 1112-9867

Available online at http://www.jfas.info

APPLICATION OF LASER IN A OPTICAL ASSEMBLY FOR CALCULATION OF DEFORMATIONS FOLLOWING THE X AND Y DIRECTIONS

Radouane Daira*, Boudjema Bouzid

Department of sciences of mater, University August 20, 1955 of skikda, Road of El Haddeik LP 26, Physico Chemistry of Surfaces and interfaces Research Laboratory of Skikda (LRPCSI), Algeria

Received: 29 April 2023 / Accepted: 17 December 2023 / Published: 26 December 2023

ABSTRACT

We present the speckle interferometry method to determine the deformation of a piece. This method of holographic imaging using a CCD camera for simultaneous digital recording of two states object and reference. The reconstruction is obtained numerically. This latest method has the advantage of being simpler than the methods currently available, and it does not suffer the holographic configuration faults online. Furthermore, it is entirely digital and avoids heavy analysis after recording the hologram. This work was carried out in the laboratory HOLO 3 (optical metrology laboratory in Saint Louis. France) and it consists in controlling qualitatively and quantitatively the deformation of object by using a camera CCD connected to a computer equipped with software of Fringe Analysis**.**

Keywords: Speckle, Non destructive testing, Interferometry, Image processing.

Author Correspondence, e-mail: daira_radouane@yahoo.fr

doi: http://dx.doi.org/10.4314/jfas.1328

1. INTRODUCTION

lectronic speckle interferometry is One method based on the coherent addition of the light scattered from the surface of the sample and a reference beam [1-3]. The phase changes in a

speckle due to movement of the object are encoded by the reference beam with the assumption that the microstructure of the object is modified. The displacement field is extracted by correlation of two models, one taken before and a shimmer taken after the object movement. The method requires the surfaces, which scatter the light. Thus the network or surface or smooth is necessary.

2. STRAIN FIELD MEASUREMENT TECHNIQUES WITH INTERFEROMETRIC METHODS

Only a few techniques provide direct stress fields which speckle interferometry is the most popular. The principle of the ESPI is interfering an optical wavefront with a shifted copy to last [4]. The resulting fringes are related to the gradient of the optical phase from which the displacements of the gradient are deducted. Strain components or local rotations are therefore directly obtained from these measurements.

Various devices have been proposed for detecting the effect of displacement [5, 6-10]. Ligtenberg proposed a method of double-exposure to measure displacement folded plates. [11] These quantities are directly proportional to the surface

stress components with the assumption Love-Kirchhoff [12]. Various optical set-up providing curvature fields are described [13].

The intensities of the figures of three interferometers interference is recorded by the CCD cameras in succession by controlling the switches. After loading a new set of interference patterns due to phase changes emerges and is recorded by the camera. By comparing the intensities before and after loading three visible fringe patterns are generated [14, 15, 16]:

$$u(x,y) = \frac{\lambda}{4\pi sin\alpha_{xoz}}.\Delta u(x,y)$$

$$v(x,y) = \frac{\lambda}{4\pi sin\alpha_{yoz}}.\Delta v(x,y) \quad (1)$$

$$w(x,y) = \frac{\lambda}{4\pi}.\Delta w(x,y) - u(x,y)sin\alpha_{xoz}$$

Where λ is the wavelength of laser, and $\Delta_u(x,y)$, $\Delta_v(x,y)$ and $\Delta_w(x,y)$ are the phase changes of two in-plane and one out-of-plane interferometers, respectively. The value of α_{xoz} and α_{yoz} represents an illumination angle in the xoz-plane and the yoz-plane, respectively. As shown in

(1), determination of three deformation components (u, v and w) needs evaluation of the phase changes [14, 17]. To calculate a phase distribution from the digitized intensity data, a phase shift technique has to be applied in the measurement system [14]. Different phase shift methods have been developed for phase calculation. Generally, they can be divided into two categories (1) a temporal phase.

shift method and (2) a spatial phase shift method. The temporal phase shift method employs multi-interference images and the spatial phase shift method uses a single image [14, 18]. Note that the temporal phase shift technique is suited for a static measurement and the spatial phase shift method is for a dynamic measurement, especially, for a transient vibration measurement. Here, since applied loads were static, the temporal phase shift technique was applied and the algorithm of four interference images was utilized [14].

3. Determination of Surface Deformations and Strains

When a sample has an extensive curved surface, a coordinate system on the object surface varies with the contour. The three deformation components on the object surface are expressed differently in the sensor coordinate. Here, the deformations components in the sensor coordinate are transformed into the object coordinate [14, 19]:

$$\begin{pmatrix} u' \\ v' \\ w' \end{pmatrix} = \begin{pmatrix} l1 & m1 & n1 \\ l2 & m2 & n2 \\ l3 & m3 & n3 \end{pmatrix} \begin{pmatrix} u \\ v \\ w \end{pmatrix} \quad (2)$$

where u, v, and w are the measured deformation components in the sensor coordinate system (xyz-coordinates), and u', v' and w' are the deformation components on the object surface (x'y'z'-coordinates). Both xyz and x'y'z' are the Cartesian coordinates. The elements of l_i, m_i and n_i are the direction cosines values between x', y' and z' axes, and x, y and z axes. After the transformation from a set of u, v and w, into the other set of u', v' and w', the in-plane strains on the curved surface are calculated [14, 20]:

$$\varepsilon_{x'x'} = \frac{\partial u'}{\partial x'} = \frac{\partial u'}{\partial x} \cdot \frac{\partial x}{\partial x'} = \frac{\partial u'}{\partial x} \cdot l_1$$
$$\varepsilon_{y'y'} = \frac{\partial v'}{\partial y'} = \frac{\partial v'}{\partial y} \cdot m_2 \quad (3)$$

$$\gamma_{x'y'} = \frac{\partial u'}{\partial y'} + \frac{\partial v'}{\partial x'} = \frac{\partial u'}{\partial y}.m_2 + \frac{\partial v'}{\partial x}.l_1$$

The surface principal strains are determined according to the principle of Mohr's circle [14]:

$$\varepsilon_{p'p''} = \sqrt{\frac{(\varepsilon_{x'x'} + \varepsilon_{y'y'})}{2}} \pm \sqrt{\frac{(\varepsilon_{x'x'} + \varepsilon_{y'y'})^2}{4}} + \gamma_{x'y'}^2 \quad (4)$$

Enter here the tsxt of second subtitle, enter here the tsxt of second subtitle, enter here the tsxt of second subtitle, enter here the tsxt of second subtitle, enter here the tsxt of second subtitle, enter here the tsxt of second subtitle, enter here the tsxt of second subtitle, enter here the tsxt of second subtitle, enter here the tsxt of second subtitle, enter here the tsxt of second subtitle, enter here the tsxt of second subtitle, enter here the tsxt of second subtitle, enter here the tsxt of second subtitle, enter here the tsxt of second subtitle, enter here the tsxt of second subtitle enter here the tsxt of second subtitle, enter here the tsxt of second subtitle enter here the tsxt of second subtitle [3].

4. EXPERIMENTAL CONDITION

This experiment was performed to Holo 3 in France, The sample (W = 20 mm) was tested in compression, but in our case we use interferometry (ESPI) and digital image correlation to measure the full field stress in the gauge area. Gradients longitudinal deformation. in the vertical direction ($\partial e_{xx}/\partial y$) were then calculated from the optical data constraint [21]:

$$e_{xx} = \frac{-6aFy}{EBW^3} = \frac{-yd}{6W^2}, e_{yy} = \frac{-vyd}{6W^2}, e_{xy} = 0 \quad (5)$$

$$\frac{\partial e_{xx}}{\partial y} = \frac{-6aF}{EBW^3} = \frac{-d}{6W^2}, \frac{\partial e_{yy}}{\partial y} = \frac{-v6aF}{EBW^2} = \frac{-yd}{6W^2} \quad (6)$$

Where: *F* is the applied load, *d* is an applied displacement to the inner loading points, *E* is the Young's Modulus of the beam material, *v* is Poisson's ratio, *W* is the width of the beam, *B* is the thickness of the beam, and *a* is the distance between the inner and outer loading points.

The co-ordinate system adopted is shown in Fig.1 [21], and the origin was chosen as the centre of the beam.

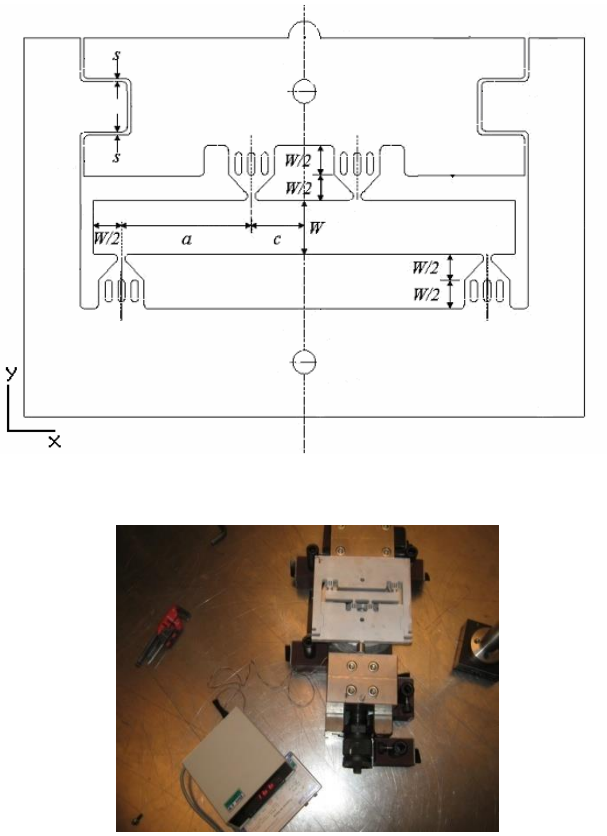

Fig. 1. Real picture of the piece

Before our experience, it is first necessary to look voltage piezoelectric, it was manually by applying voltages and calculation of displacement to get the curve descriptive of the piezoelectric, but this manipulation research of the curve is done directly with the Fringe Analysis software gives us the following figure:

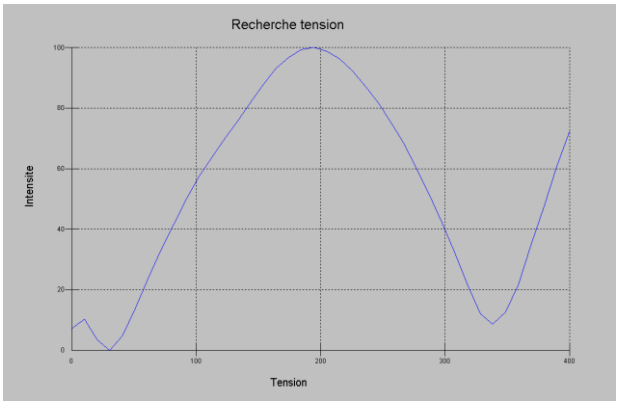

Fig. 2 Calibration curve of the piezoelectric

After calibration of the piezoelectric you go to install our assembly, it is sensitive to movements in both directions (along x and y), and for this we used a laser that emits green light and having a power having until 20 w (in our experiment we used a power of 1 w, which was sufficient for the smooth handling) [22].

5. EXPERIMENTAL DEVICE

The assembly is composed of four spherical mirrors used to focus the laser light on our part, which is fixed in a cavette which serves to apply forces with the force sensor with a 1 KN, they allow the assembly to be sensitive in both directions (x and y), mirrors have the following coordinates:

M_1 (-1030, -135, 240), M_2 (0, 940, 240), M_3 (1040, -120, 240), M_4 (0, -1 180, 240), and another mirror which is mounted on a piezoelectric to assured the phase shift of π / 2, the assembly is connected with a CCD camera that tracks the distortions of the play in real time and Fringe Analysis software that allows the processing of the results.

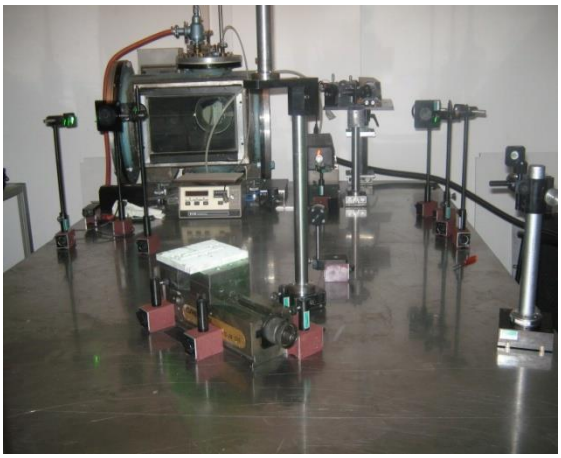

Fig.3. Image of the experimental setup used for the calculation of bending deformation of a room

6. RESULTS

We begin by deforming the part by applying forces with a 1 kN, and we follow the evolution of our first deformation along the x axis. The results are shown in the figure above.

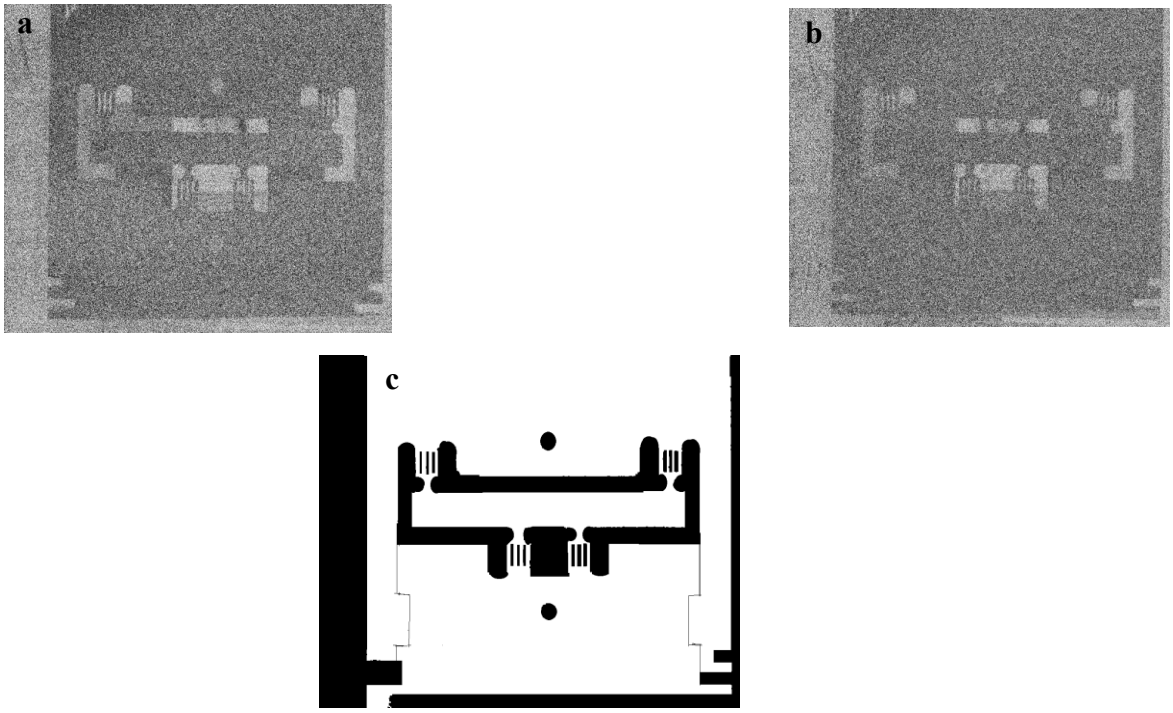

Fig.4. a- baseline Image; b- Image deformed state, c- mask used for processing the interferograms

The specklogrammes obtained for different strains along the X axis are shown by the figure (5).

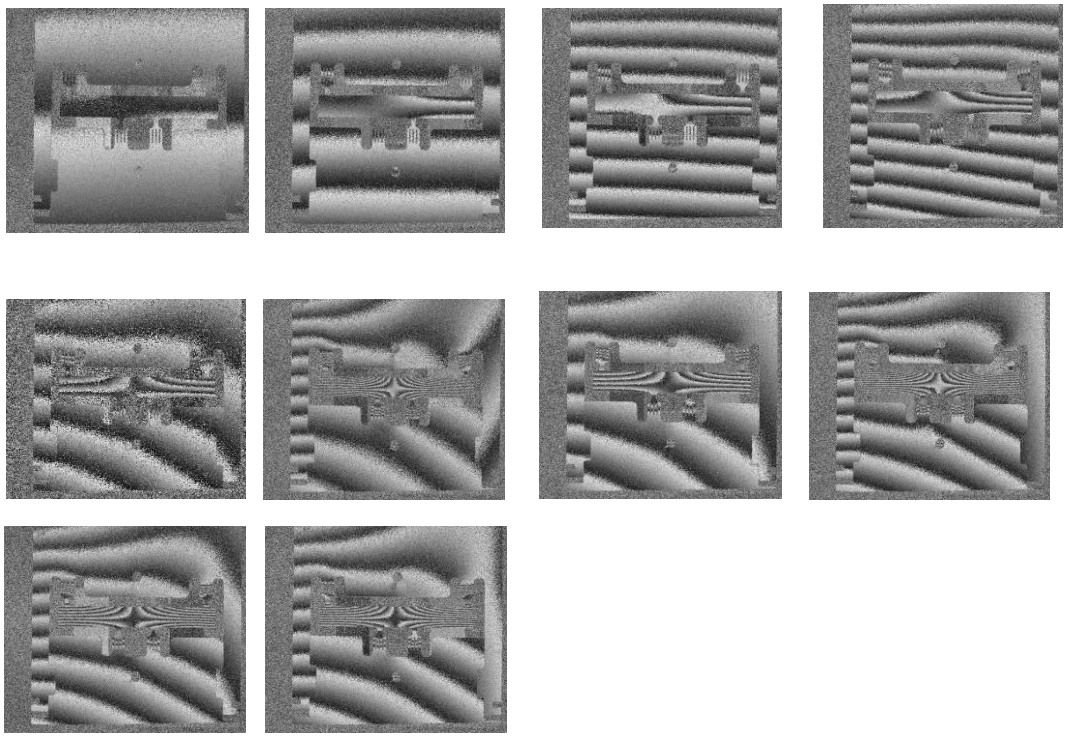

Fig.5. Specklogrammes show the deformation of the piece subjected to bending by a stepping force of 1 KN

On observing the results either in the direction of deformation along X or Y following, we note that the interfringes decreases when increasing strength, and it is readable on our interferograms, but the problem for the form difficult to our room is the observation curved fringes indicate that our part undergoes a small rotation during application of our strength and to address this issue in order to properly calculate our displacement vector.

6.1. Calculating unwrapping phase

After one pass for calculating the wound stage for different values of the force F:

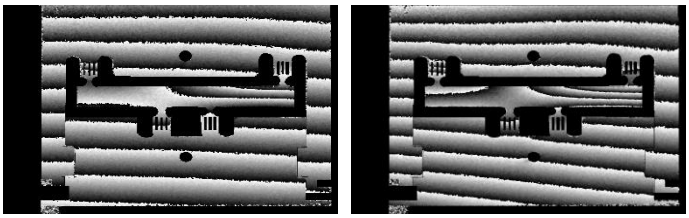

Fig.6. Phase unwrapping by applying force F KN = 3, F = 4 kN

6.2. Calcul of stress and deformation

The same software allows us to calculate the various internal constraints of our room and the achieved distortion.

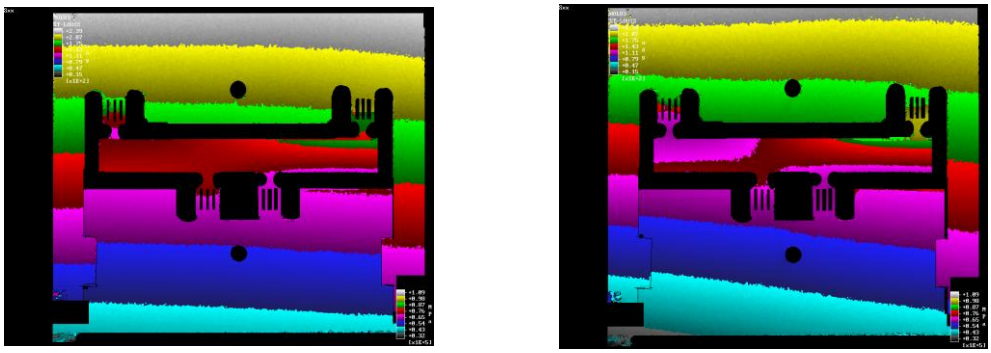

Fig.7. Specklogrammes show the different internal stresses of the room KN F = 3, F = 4 KN

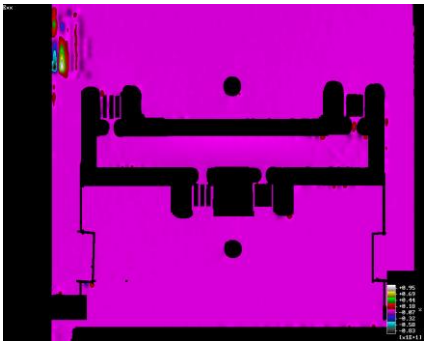

Fig.8 . Specklogramme shows the deformation zones in the room

From the cuts made, measure the deformation and displacement applied depending on the load (we interress to the X direction). The test was repeated several times, the sample undergoes deformations of 1 KN not. The results obtained for the displacement relative to load are shown in Fig 9.

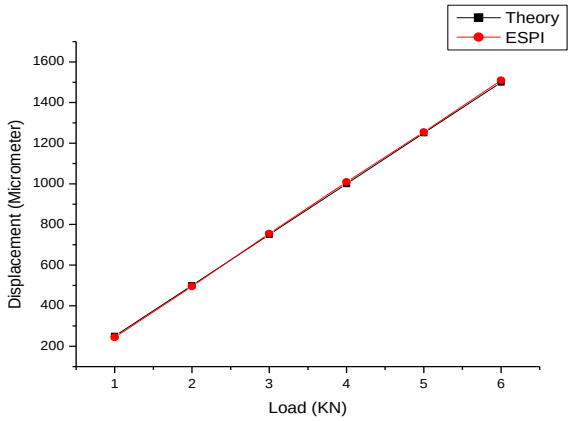

Fig.9. Results obtained for applied displacement versus load for three repeat tests

Although the measures were closer to the theoretically predicted response when compared to the previous model, the dispersion in the data acquired during the three repeat points was significantly increased. This was attributed to the low thickness of the sample that is to say it has become more difficult to align vertically in the compression plates but it did no way to prevent find practical results closer than that obtained with ESPI technique.

we made a small program with Matlab, and it was not our software to calculate the rotation value is beyond our calculation.

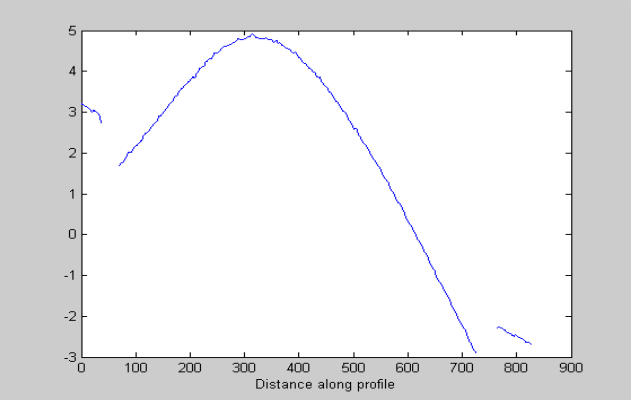

Fig.10. Curve shows the continuity of the unwrapped phase

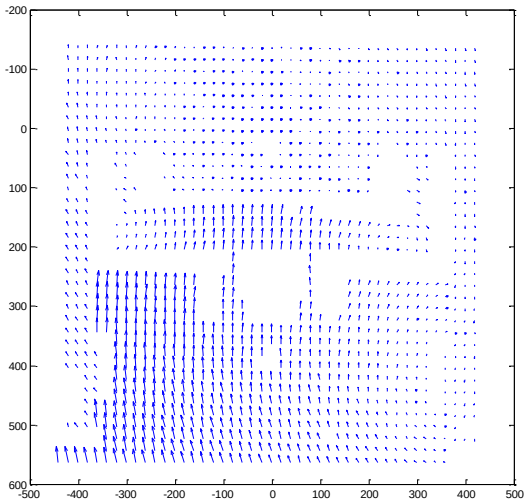

Fig.11. Workpiece motion vector obtained by the Matlab program

7. CONCLUSION

Digital speckle interferometry (DSPI) can make the whole area, the microscopic deformation measurements with high resolution without contact for the determination of 3D stress distributions. Through the development of a piezoelectric device and the measurement on loading and a new calibration system of force versus DSPI, we constructed an advanced and integrated DSPI system local contour information to data deformation. Using a Fringe analysis software, we determined 2D distributions of stress and discussed efficiency and limitations of the system described.

8. REFERENCES

[1] Dainty JC, Laser speckle and related phenomenon, Berlin: Springer; 1984.

[2] Jones R, Wykes C, Holographic and speckle interferometry, Cambridge, MA: Cambridge University Press; 2000.

[3] Robinson DW, Reid GT, Interferomgram analysis: digital fringe pattern measurement techniques, Philadelphia, PA: IOP Publications Ltd; 2001.

[4] Krishnaswamy S. Techniques for non-birefringent objects: coherent shearing interferometry and caustics. In: Rastogi PK, editor. Photomechanics, topics applied physic 77. Berlin: Springer; 2000.p. 295–321.

[5] Bulhak J, Surrel Y. Grating shearography. In: Interferometry ‘99: Techniques and Technologies, 20–23 September, Pultusk, Poland, vol. SPIE 3744.; 1999. p. 506–15.

[6] Ronchi V. Forty years of history of a grating interferometer. Appl Opt 1964;3:437. Optical Society of America.

[7] Wyant JC. Double frequency grating lateral shear interferometer.Appl Opt 1973;12:2057. Optical Society of America.

[8] Patorski K. Talbot interferometry with increased shear. Appl Opt 1985;24:4448. Optical Society of America.

[9] Tippur HV, Krishnaswamy S, Rosakis AJ. Optical mapping of crack tip deformations using the methods of transmission and reflection coherent gradient sensing: a study of crack tip K-dominance. Int J Fract 1991;52:91. Kluwer Academic Publisher.

[10] Lee HS, Krishnaswamy S. A compact polariscope and shearing interferometer for mapping stress fields in bimaterial systems. Exp

[11] Ligtenberg FK. The moire´ method. In: Proceedings of SESA, vol. 12.; 1954. p. 83–98.

[12] Timoshenko S, Woinowsky-Krieger S, Theory of plates and shells, New York: McGraw-Hill; 1958.

[13] Kao TY, Chiang FP. Family of grating techniques of slope and curvature measurements for static and dynamic flexure of plates. Opt Engng 1982;21(4):720–42.

[14] L.Yang and al, ‘Measurement of Strain Distributions in Mouse Femora with 3D-digital speckle pattern interferometry’, Opt Lasers Eng. Aug 2007; 45(8): 843–851.doi: 10.1016/j.optlaseng.2007.02.004

[15] Yang L, Steinchen W, Schuth M, Kupfer G. Precision measurement and nondestructive testing by means of digital phase shifting speckle pattern and speckle pattern shearing interferometry. Measurement. 1995;16:149–160.

[16] Bown B, Martin S, Toal V, Langhoff A, Whelan M. Dual in-plane electronic speckle pattern interferometry system with electro-optical switching and phase shifting. Applied Optics. 1999;38(4):666–673.

[17] Creath K. Phase-shifting speckle interferometry. Appl. Opt. 1985;24(18):3053–3058.

[18] Kreis T. Holographic Interferometry: Principles and Methods. John Wiley & Sons, Inc;

1996

[19] Fung YC. A First course in continuum mechanics: for physical and biological engineers and scientists. Prentice Hall, Englewood Cliffs; NJ: 1994.

[20] Zhang P, Tanaka SM, Jiang H, Su M, Yokota H. Diaphyseal bone formation in murine tibiae in response to knee loading. J. Appl. Physiol. 2006;100:1452–1459.

[21] E.Patterson, Project acronym: SPOTS 'Standardisation Project for Optical Techniques of Strain Measurement',January 2006.

[22] R. Daira**,** B. Boudjema 'Application of optical method in chemical processus as corrosion', phys.chem.news PCN, volume 68, pp 36-41.2013.